IOP PUBLISHING
IOP FTC
JOURNAL OF PHYSICS D: APPLIED PHYSICS
J. Phys. D: Appl. Phys. **41** (2008) 102001 (4pp)
doi:10.1088/0022-3727/41/10/102001

FAST TRACK COMMUNICATION

Formation of reconfigurable optical channel waveguides and beam splitters on top of proton-implanted lithium niobate crystals using spatial dark soliton-like structures

Yang Tan[1], Feng Chen[1,4], Xue-Lin Wang[1], Lei Wang[1], V M Shandarov[2] and D Kip[3]

[1] School of Physics, Shandong University, Jinan 250100, People's Republic of China
[2] Department of Quantum Electronics, State University of Control System and Radioelectronics, Tomsk 634050, Russia
[3] Institute of Physics and Physical Technologies, Clausthal University of Technology, Clausthal-Zellerfeld 38678, Germany

E-mail: drfchen@sdu.edu.cn

Received 30 January 2008, in final form 17 March 2008
Published 8 April 2008
Online at stacks.iop.org/JPhysD/41/102001

Abstract
We report on the formation of reconfigurable optical channel waveguides (including straight stripes and Y-branches) on top of iron-doped lithium niobate crystals. The sample surface is first implanted by 500 keV protons to form a planar waveguide showing a propagation loss of $\sim$1.6 dB cm^{-1} after modest post-implantation annealing. Afterwards, the sample surface is illuminated with well-defined stripe patterns (straight channels, beam splitters) of green light using lithographic masks. Due to the photovoltaic effect in lithium niobate resulting in negative index changes in illuminated regions, waveguide layers are formed in the non-illuminated regions perpendicular to the planar waveguide in the same way as it occurs in the dark spatial soliton regime. In this way two-dimensional waveguides are formed in the overlap region on top of the crystal that may be used for reconfigurable optical interconnections and splitters.

(Some figures in this article are in colour only in the electronic version)

1. Introduction

Lithium niobate ($LiNbO_3$) is a well-known optical crystal for versatile photonic applications due to the combination of excellent performance of various properties and low cost [1]. When doped with iron, this material ($Fe:LiNbO_3$) exhibits attractive photorefractive features, which can be used for certain promising applications, e.g. signal amplification, data storage or phase conjugation [2]. Optical waveguides enable the confinement of light in one or two dimensions to small regions, i.e. in planar or channel/ridge waveguide configurations, reaching high optical intensities even at low input powers, which brings out considerable improvement of related properties with respect to the bulk [2, 3]. In particular, excellent nonlinear features with fast response times have been realized in photorefractive waveguides [2, 4–7]. In addition, two-dimensional (2D) waveguides, usually with better confinement of light than for planar 1D geometries, can be easily connected with integrated photonic components in optical systems, allowing for the construction of complicated optical circuits for diverse applications [8].

[4] Author to whom any correspondence should be addressed.

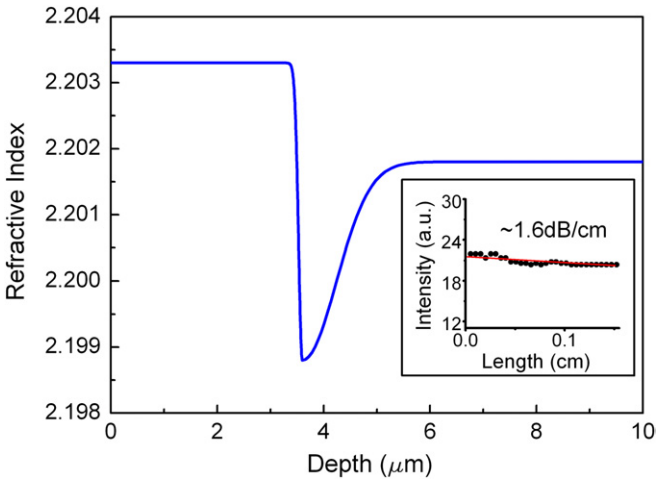

Figure 1. Refractive index profile n_e of the 500 keV proton-implanted Fe : $LiNbO_3$ waveguide after annealing at 400 °C for 30 min in air. The inset shows the waveguide loss measurement data (scattered light intensity versus propagation length).

As one of the most efficient techniques for material-property modification, ion implantation has shown its unique ability for alteration of surface refractive indices of a large number of optical materials for waveguide formation [9, 10], including Fe : $LiNbO_3$ [11]. Alternatively, permanent waveguides in Fe : $LiNbO_3$ have been fabricated by, e.g. titanium in-diffusion or proton exchange [2, 12]. In addition, Fe : $LiNbO_3$ is a self-defocusing material with saturable nonlinearity, which allows for dark spatial soliton formation through the photovoltaic mechanism [13–15]. This also paves an efficient way to optically induce channel waveguides in a planar waveguide substrate by applying additional 1D dark soliton formation with adequate masking in a perpendicular plane. For this process, in Fe : $LiNbO_3$, no external electrical field is required, as it is the case for materials with screening nonlinearity like SBN [16]. In such a configuration, the confinement of light in two dimensions is attributed to both the planar waveguide (along the surface normal) and the optical inhomogeneity formed by soliton-like light structures (laterally). Couton *et al* reported single-mode channel waveguide formation in Fe : $LiNbO_3$ on top of a titanium-diffused slab waveguide by using photovoltaic solitons [15]. In this letter, we demonstrate, to our knowledge for the first time, reconfigurable 2D channel waveguides and integrated beam splitters (Y-branches) on a proton-implanted Fe : $LiNbO_3$ planar waveguide through light induction of spatial dark soliton-like structures [17][5].

2. Results and discussion

The x-cut Fe : $LiNbO_3$ sample (0.1 mol% doping) used in our work has dimensions of $1.5(x) \times 8(y) \times 10(z)$ mm^3 and

[5] Formation of a fundamental dark screening soliton requires a π phase jump at the beam's centre, while a dark notch with uniform phase profile leads to splitting into a pair of anti-phased dark solitons (a 'Y-junction soliton', see, e.g. [17]. However, as this splitting requires propagation of the beam for several diffraction orders, this instability is not observed in our experiments.

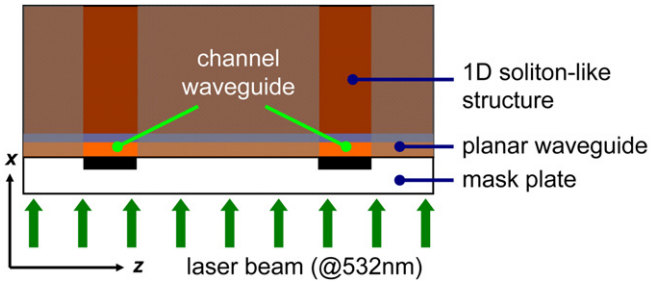

Figure 2. Schematic plot of the experimental setup for channel waveguide formation.

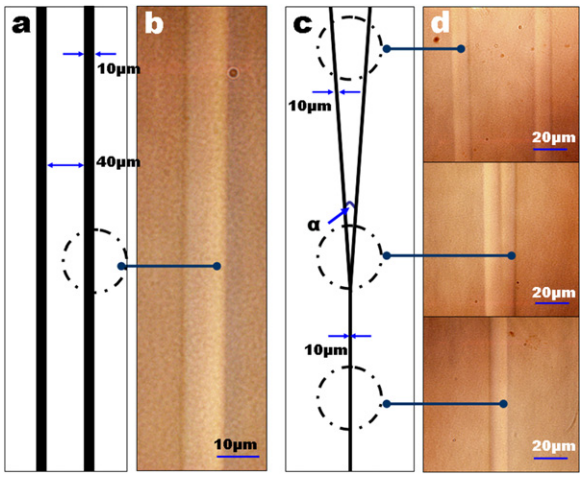

Figure 3. Lithographic mask patterns of (a) straight stripe and (c) Y-branch waveguides ($\tan(\alpha) = 0.01$); and microscopy photographs of the top view of (b) straight channel and (d) Y-branch waveguide, imaged by using polarized light reflection (Olympus BX51M).

is optically polished. Proton implantation (at an energy of 500 keV and a dose of 2×10^{16} cm^{-2}) is performed onto the 8×10 mm^2 face to form planar waveguide structures. A post-implantation thermal annealing at 400 °C for 30 min in air is used to remove irradiation-induced colour centres or point defects inside the planar waveguide, thus reducing damping of guided light. With this processing the planar waveguide is confined by an enhanced refractive index well (during the path of the ion trajectory) and an optical barrier with reduced index (at the end of the ion track), as shown in figure 1 for the extraordinary refractive index (n_e) profile (reconstructed by the reflectivity calculation method [18] based on the m-line spectroscopy). The propagation loss of the waveguide is determined to be ~1.6 dB cm^{-1} via the scattering detection technique [19].

The channel waveguides are written on top of the planar waveguide surface by photolithographic mask modulated light patterns. Figure 2 depicts the schematic plot of the light-induction process to form 2D channels. The mask consisting of specially designed patterns (stripes and Y-junctions) is in close contact with the bottom face of the planar waveguide sample. A linearly polarized green light beam (wavelength of 532 nm, polarization along the c-axis of the crystal) passes the mask from the back side and illuminates the whole sample, while keeping some stripe-like regions unexposed. Since

Fe : $LiNbO_3$ possesses a strong self-defocusing (photovoltaic) effect, light exposure results in a negative refractive index change in the illuminated regions. Therefore, in the dark regions (narrow stripes) 1D spatial dark soliton-like structure will form, resulting in non-diffractive light propagation along these stripes within a host planar waveguide. After several diffraction lengths (∼50 μm) these structures become unstable and evolve into Y-junctions [17][5]; however, this does not affect the channel waveguide formation within the relatively thin planar waveguide layer (with thickness of ∼3.3 μm). In our experiments, the illumination through the mask lasts 40 min at an average intensity of 7.3 mW cm^{-2}, resulting in an induced negative index change of ∼0.0008 (measured by the prism coupling method) in the exposed regions.

Two types of chromium-glass masks are used in our experiments. One comprises a series of 10 μm wide straight chromium stripes separated by 40 μm wide open regions transparent to the light, see figure 3(*a*). In another mask, Y-junction patterns are constructed by the chromium films, leaving the surroundings transparent to the light (figure 3(*c*)). Figures 3(*b*) and (*d*) show microscopy photographs of the top view of the induced straight channel waveguides and the formed beam splitter, respectively. As one can see, both structures are clearly visible and in accordance with the related mask patterns. The superposition of the planar waveguide index profile and the light-imprinted dark soliton-like index structures can be seen in figure 4.

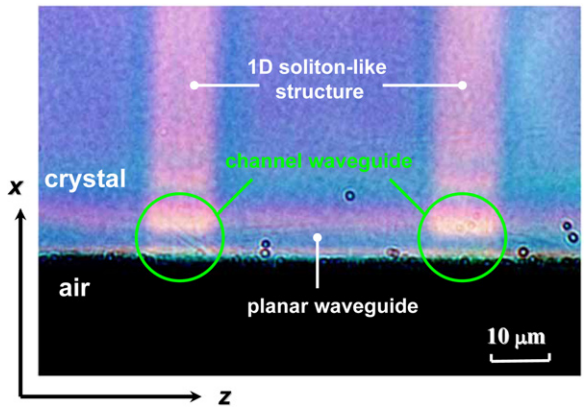

Figure 4. Superposition of the refractive index profile of planar layer and light-imprinted (1D dark soliton-like) stripes, imaged from the sample's entrance facet when illuminated by polarized light.

To investigate the light propagation in the light-induced 2D waveguides, a He–Ne laser beam (wavelength of 632.8 nm) is launched into the channels through a typical end-facet coupling arrangement [20]. At this wavelength, the photosensitivity is low, and the maximum light intensity without optical erasure is ∼3.7 W cm^{-2}, which is much larger than the writing intensity of 7.3 mW cm^{-2} at a wavelength of 532 nm. Figures 5(*a*) and (*b*) show the near-field intensity distributions of the straight channel and the Y-junction, respectively, measured directly from the output facet of the samples. As one can see, the channel waveguides are single-mode, carrying light in a well-confined way. In addition, the photo-induced Y-branch splits the incident light into two parts with a splitting ratio close to 1 : 1, which exhibits good performance.

To obtain a better understanding of the photo-induced channel waveguides, we apply a numerical simulation of the light propagation based on the finite difference beam propagation method (FD-BPM) [21]. The stationary 2D refractive index distributions of the channel waveguide cross sections are reconstructed by considering the longitudinal planar waveguide index profile and the lateral index modulations induced by the light illumination, i.e. a superposition of the index changes of proton implantation and the photo-induced index perturbation (as shown in figures 5(*e*) and (*f*)). By comparing figures 5(*a*) and (*b*) with (*c*) and (*d*) (indicating the calculated modal intensity profiles), we may conclude that there is a reasonable agreement between numerical and experimental data, which allows for the modelling of tailored channel waveguide structures through optical induction.

Another important feature of the photo-induced patterns is that index changes can be erased when the sample is exposed to white light (e.g. in our experiment, a cold white-light lamp at 100 W is utilized to illuminate the sample surface for 30 min to erase the channel waveguides), allowing for reconfiguration of channel waveguide devices. On the other hand, without such

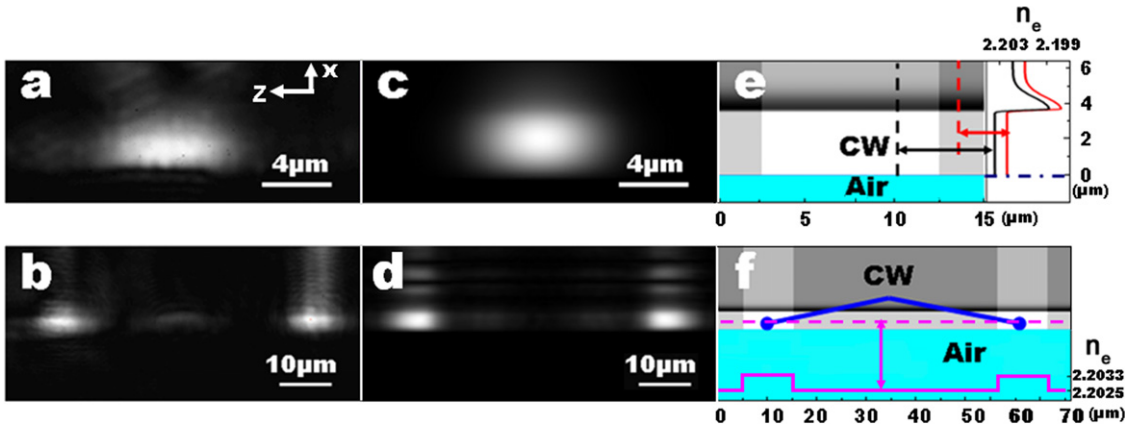

Figure 5. Near-field intensity distributions of (*a*) straight channel and (*b*) Y-branch waveguides; calculated light intensity profiles from the output facet for (*c*) straight channel and (*d*) Y-branch waveguides; reconstructed 2D index distributions of straight channel (*e*) and Y-branch waveguide (*f*) at the output-face cross section. The wavelength of light is 632.8 nm. CW: channel waveguide.

illumination, the relaxation time of light-induced structures can be estimated to be of the order of a few weeks.

3. Conclusion

In conclusion, we report on the formation of reconfigurable channel waveguides on top of proton-implanted Fe : $LiNbO_3$ planar waveguides using the spatial dark soliton-like structures imprinted with light. The calculated modal distributions show good agreement with the measured near-field intensity profiles of the light, which allows for the design of reconfigurable devices for optical communications, e.g. optical interconnections and routers, using near-infrared wavelengths where the material's photosensitivity is negligible.

Acknowledgments

This work is carried out with the financial support of the National Natural Science Foundation of China (Grant No 10505013), the associated NSFC-RFBR project (Grant No 10711120169), and RFBR (Project No 06-02-39017). F Chen also thanks SRF for ROCS, SEM.

References

[1] Arizmendi L 2004 *Phys. Status Solidi* a **201** 253
[2] Kip D 1998 *Appl. Phys.* B **67** 131
[3] Mackenzie J I 2007 *IEEE J. Sel. Top. Quantum Electron.* **13** 626
[4] Fluck D, Pliska T, Günter P, Beckers L and Buchal C 1996 *IEEE J. Quantum Electron.* **32** 905
[5] Dazzi A, Mathey P, Lompré P, Jullien P, Moretti P and Rytz D 1999 *J. Opt. Soc. Am.* B **16** 1915
[6] Mathey P, Dazzi A, Jullien P, Rytz D and Moretti P 2001 *J. Opt. Soc. Am.* B **18** 344
[7] Kip D, Kemper B, Nee I, Pankrath R and Moretti P 1997 *Appl. Phys.* B **65** 511
[8] Lifante G 2003 *Integrated Photonics: Fundamentals* (New York: Wiley)
[9] Townsend P D, Chandler P J and Zhang L 1994 *Optical Effects of Ion Implantation* (Cambridge: Cambridge University Press)
[10] Chen F, Wang X L and Wang K M 2007 *Opt. Mater.* **29** 1523
[11] Dazzi A, Mathey P, Lompré P, Jullien P, Odoulov S G and Moretti P 1999 *J. Opt. Soc. Am.* B **16** 256
[12] Kip D, Bartholomäus T, Garcia P M and Krätzig E 1994 *J. Opt. Soc. Am.* B **11** 3
[13] Shandarov V, Kip D, Wesner M and Hukriede J 2000 *J. Opt. A: Pure Appl. Opt.* **2** 500
[14] Rosberg C R, Neshev D N, Krolikowski W, Mitchell A, Vicencio R A, Molina M I and Kivshar Y S 2006 *Phys. Rev. Lett.* **97** 083901
[15] Couton C, Maillotte H, Giust R and Chauvet M 2003 *Electron. Lett.* **39** 286
[16] Kip D, Wesner M, Shandarov V and Moretti P 1998 *Opt. Lett.* **23** 921
[17] Chen Z, Mitchell M and Segev M 1996 *Opt. Lett.* **21** 716
[18] Chandler P J and Lama F L 1986 *Opt. Acta* **33** 127
[19] Goell J E and Standly R D 1969 *Bell Syst. Technol. J.* **48** 3445
[20] Chen F, Wang L, Jiang Y, Wang X L, Wang K M, Fu G, Lu Q M, Rüter C E and Kip D 2006 *Appl. Phys. Lett.* **88** 071123
[21] Yevick D and Bardyszewiski W 1992 *Opt. Lett.* **17** 329